FATIGUE STRENGTH OF CROSS GIRDER CONNECTIONS CONSTRUCTED WITH 9% Ni STEEL PLATE

K. Tanaka and S. Matsuoka*

INTRODUCTION

A large proportion of minor fractures in engineering structures arise from design details and some very serious fractures have originated at such details. It is needless to say that close attention to detail design is sufficiently rewarding. Considerable improvements in detail design have been made in recent years and the stress situation in such details can now be estimated reasonably accurately by means of the finite element method (FEM). In a previous work in NRIM, the fatigue strength of steel beams with bracket plates welded to the tension flange was examined with particular attention to the bracket design [1]. It was revealed that crack initiations from such design details were successfully predicted from the results of simulation tests on plate specimens with fillet welds by utilizing the stresses at the corresponding positions. These stresses were measured by means of electric resistance strain gages or calculated by FEM. In this study the fatigue strength of cross girder connections was investigated. These girders were planned to serve in the fabrication of a LNG ship in Sasebo Heavy Industries Co., and were similar to the beam structure tested in the previous study [1]. The main objective of the present study is to establish an instructive guide for the determination of design stress at the details in such complicated structures. The fatigue behaviours were analyzed with respect to the stress states in the beam details, the stresses being computed by FEM. In addition, the fatigue behaviours were compared with the fatigue strengths of plate specimens with various types of welding attachments similar to those used in the beams.

TEST SPECIMENS AND TEST PROCEDURES

All beam and plate specimens were fabricated from 10mm thick 9 per cent Ni steel (ASTM553A-71) plate. The chemical analysis of the material and the mechanical properties are shown in Table 1. The beam specimens were composed of two beams of 500mm and 175mm depths joined at right angles and welded on a bottom plate. The dimensions of the specimens and the details at the intersection of both beams are shown in Figure 1. A slot was made in the main beam web where the upper flange of the cross beam intersected it. The buckling of the main beam was prevented by a web stiffener setting on the upper flange of the cross beam. The beam specimens were classified in two series. Type 1 beams had a backing bracket plate welded on the upper flange of the cross beam opposite to the stiffener and Type 2 beams did not. All the fillet welds were made manually in the horizontal position by using Inconel electrodes. Testing was carried out in bending on a 0.5MN Shimadzu electro-hydraulic machine at 1 - 5Hz, the main beam being supported and the cross beam loaded as il-

*National Research Institute for Metals, Tokyo, Japan.

lustrated in Figure 1. In all tests the load cycle varied from a minimum value of 0.02MN to a maximum one between 0.17MN to 0.39MN. Tests were stopped when a crack was found to originate from the slot in the main beam or when specimens survived 2 x 10^6 cycles.

Five series of plate specimens were used in the comparative tests, full details of which are shown in Figure 2. These were plain plate specimens, longitudinal non-load-carrying fillet welds and three different types of transverse load-carrying fillet welds. The welding was performed in the same method as that for the beam specimens. Plate specimens were tested under zero-to-tension loading in a 0.15MN MTS electro-hydraulic testing machine at 20Hz.

FEM ANALYSIS

In order to examine the effect of reinforcement by stiffener and bracket, the stress states were analyzed for three cases of cross girder connections; one with both attachments (Type 1), one with stiffener only (Type 2), and one without any such attachment. The computation was conducted in Sasebo Heavy Industries Co. The element type used was a well-established four node plane stress element. The specimen was assumed to be fixed at AA' section and free at the support line SS' (Figure 1). The effect of shape change associated with the fillet welds was not taken into account. The distributions of principle stresses thus obtained are represented in Figure 3 for the stiffener and bracket in Type 1 beam specimen and for the stiffener in Type 2. The accuracy of the calculation was checked by comparing the computed results with those of measurement by means of strain gages positioned on the inner side of the stiffener and bracket for all of the specimens tested (arrow marks in Figure 3). These two results gave an excellent fit within an error of ±5 per cent. The calculated values of the maximum principle stress in the meshes relevant to the positions designated in Figures 3 and 4 are shown in Table 2 for two types of beam specimens at 0.1MN loading. It is apparent from Figure 3 that in the case of Type 1 beam specimen the stresses in both stiffener and bracket were distributed almost evenly. The greatest magnitudes of principle stress were obtained at both ends of the bracket, that is at positions B1 and B2 in Figure 3. The elimination of the bracket made the stress in the stiffener less uniform. Namely, the force in the stiffener of Type 2 specimen was concentrated at the root of the inner side of the stiffener (position S1) and the corresponding stress value was higher than the maximum one for Type 1 specimen as shown in Table 2. The FEM calculation also revealed that the magnitude of principal stress around the slot (position SL in the illustration in Figure 4) was affected by the attachments, for Type 2 being about twice as large as that for Type 1. Furthermore, it was derived from the results of FEM calculation for the plain cross girder structure with no attachments that the values of stress in the main beam web were only 10 per cent larger than those for Type 2 specimen. These facts suggest that the web stiffener was effective for the reinforcement of main beam web only when this was backed by the bracket from the opposite side of the web.

FATIGUE TEST RESULTS

Typical fatigue behaviours in a Type 1 beam specimen tested at the load range of 0.37MN are shown diagrammatically in Figure 4. The fatigue cracking in the beams took place in the following sequence. (1) The

crack started from the toe of the fillet weld at the lower bracket end (position B1) and then it propagated along the weldment at the bracket/cross beam flange junction, followed by the separation of the bracket from the flange. Alternatively, in some other specimens, cracks originating from the upper bracket end (position B2) resulted in the separation of the bracket from the main beam web. Once the bracket plate separated from the cross girder or the main beam, the situation for Type 1 specimens was essentially identical to that for Type 2 specimens and hence the following processes of failure occurred in a similar manner for both types of specimens. (2) The crack started from the toe of fillet weld at the root of inner side of the stiffener (position S1) and then propagated along the weld at the stiffener/cross girder flange junction. However, in this mode the growth rate of crack was so slow that the crack sometimes stopped propagation in the intermediate portion of the junction. (3) A crack initiated from the toe of the fillet weld on the main beam web at the corner between the cross girder web and the bottom plate (position W). This extended both in the horizontal and vertical directions along the welds at the junctions of main beam web/bottom plate and cross girder web, respectively. (4) The final failure occurred from the slot in the main beam with cracks being initiated just at the positions where the stresses were assessed by FEM to be maximum (position SL) and propagated in the direction perpendicular to the maximum principle stress. The tests were stopped shortly after the initiation of this mode of crack was detected.

The lives at crack initiation for the four modes of failure in the two types of beam specimens are shown against applied load range in Figure 5. The crack initiation was identified by inspection with the naked eye. At this stage most of the cracks were between 5mm and 10mm in length. The data in each of the failure modes for each of the two specimen types seemed to have a systematic dependence on load range. The slopes for the two curves of primary crack initiation, one for cracks originating in the bracket of Type 1 specimens (empty circles) and the other for those in the stiffener of Type 2 specimens (filled triangles), are just coincident with each other. The corresponding endurance at a given load range differed by a factor of six between the two curves. It is also obvious in Figure 5 that the fatigue strengths of the main structure were markedly improved by the attachment of the backing bracket. Namely, the lives at initiation for cracks at positions W and SL increased by a factor of four and two, respectively, in Type 1 beam specimens compared with those in Type 2 beam specimens. The differences were mainly due to the lives exhausted until the complete separation of the bracket plate in Type 1 beams.

DISCUSSION

The relationships between the life at initiation of various modes of cracks and the applied load range are replotted from Figure 5 in the form of an SN curve in Figure 6. The relevant stress ranges were assessed by referring to the values of the maximum principle stresses given in Table 2. The results for cracks present in the bracket (empty circles) were derived from the data for Type 1 beams and the others from those for Type 2 beams. It is evident from Figure 6 that the results for the three modes of cracks associated with the fillet welds of the beam specimens were expressed consistently by an SN curve. As was expected, the fracture starting from the corner of the slot resulted in much higher fatigue life than that at the welded positions.

The results for the various types of plate specimens are plotted by filled marks in Figure 6. The tests for T2, T3 and T1 and P types of plate specimens were intended to simulate the fractures appearing in the beams at the locations of B1 (or B2), S1, W and SL, respectively. The stress ranges for plate specimens except Type T3 were nominal ones, and those for T3 specimen were obtained by magnifying three times the nominal values. The data for three types of fillet weld, Types T2, T3 and L, in Figure 6 agreed well with each other, whereas those for Type T1 specimen gave fairly lower strength than the other three types of plate specimen. The different levels of strength were attributed to the different modes of failure; the former fillets failed from the weld toe and the latter from the weld root [1].

It is seen in Figure 6 that the data for the failure life of the welded plate specimens fracturing at the weld toe compared very well with the results of crack initiation at positions S1, B1 and W in the beam specimens. This is quite reasonable because examination of all the corresponding fillet welds in beam specimens revealed that the failure occurred at the weld toe and the propagation life in the plate specimens was negligible compared with the life at initiation. Thus it may be deduced that the life at initiation in the welding attachments of the beam specimens can be accurately predicted from comparative test results on plate specimens with similarly welded fillets. Furthermore, the fact that the fatigue lives were not dependent on the types of fillet welds suggests that one series of comparative tests on the standard type of longitudinal fillet weld, Type L in Figure 2, would suffice as a representative of all tests of the various types of fillet welds. In fact, the mean SN curve for longitudinal non-load-carrying fillet weld analyzed on the results of 179 specimens by Gurney and Hicks [2] (dotted curve) was in close agreement with the results of the beam specimens. This fact implies that the 'master curve' of fillet welds being constructed from the results of many laboratory specimens, can be adopted as the basis for design. However, care should be taken for the failure of the load-carrying type fillet, since the possible crack initiation from the weld root may reduce the strength somewhat below the master curve. Although in the case of this study the fracture in the pertinent type fillet (position W) originated from the weld toe, the most conservative design for such welded details should be based on the results for the load-carrying transverse fillet of Type T1 as exhibited in Figure 6.

The prediction of the fatigue life in the beam specimens at locations other than the fillet weld seemed difficult (position SL). It is apparent from Figure 6 that the results for plain plate specimens (Type P) provided higher strength than those for cracks starting from the corner of the slot in the beam specimens. However, when the plain plate specimens were notched about 0.3mm in depth and in root radius at the four corners of the gage part (Type PN) [3], the resulting strengths decreased to the same level as those for the slot as is shown in Figure 6. The same tendency was demonstrated in the test results on rolled beams conducted in NRIM [3]. These facts suggest that in such practical structures the strength of the smooth part was inevitably affected by some unavoidable defects. The dash-dotted curve indicated in Figure 6 is the mean curve for the failure life of plain rolled beams tested by Hirt et al. [4], and the data of this study fall in the conservative side. Thus it is recommended that this curve be taken as the master curve for designing such a smooth part as the corner of the slot.

The SN curve for fillet welds in beam specimens as shown in Figure 6 gives the fatigue strength of 98MPa at 2×10^6 cycles. On the basis of this value, the load ranges of primary crack initiation at 2×10^6 cycles were obtained by referring to the pertinent values in Table 2 as 0.13MN for Type 1 and 0.081MN for Type 2. According to the previous study [1], the crack initiation from the bracket plate was possibly impeded by changing the straight taper of bracket side-ends into such a rounded shape as was seen in the fillet of the stiffener in this study (Figure 1). In this case, the primary crack in Type 1 beam specimen would start from the weld toe location on the flange of the cross beam at the root of the inner side of stiffener (position S1) or bracket (opposite to position S1) and propagate transversely the flange. From the FEM calculation, the stresses at the relevant locations in the flange were assessed to be 49MPa at 0.1MN loading. Thus the resulting load at primary crack initiation in Type 1 specimens at 2×10^6 cycles was expected to reach 0.20MN by the rounding of the bracket side-ends.

CONCLUSION

1) The lives at the initiation of cracks in the cross girder connections were estimated with sufficient accuracy by relating the stress values calculated by FEM to the results of simulation tests on plate specimens. The relevant values of stress used were the maximum principle stresses at the locations where the crack-initiating weld toe would be positioned. The calculation was conducted without taking into account the effect of weld shape.

2) The backing plate located opposite to the web stiffener improved considerably the fatigue strength of the welded structure. It is suggested that this reinforcing effect will be almost doubled if the crack initiation from the side-ends of the bracket is impeded by changing the configuration.

ACKNOWLEDGEMENT

It is acknowledged that this study was conducted under a research contract with Sasebo Heavy Industries Co.

REFERENCES

1. TANAKA, K., MATSUOKA, S., KAWAHARA, M. and IWASAKI, N., submitted to the Engng. Fract. Mech.
2. GURNEY, T. R. and HICKS, J. C., Offshore Technology Conference, Paper OTC A907, 1973.
3. TANAKA, K. and MATSUOKA, S., Engng. Fract. Mech., 7, 1975, 79.
4. HIRT, H., YEN, B. T. and FISHER, J. W., J. Struc. Div. ASCE, 97, 1971, 1879.

Table 1

Element	C	Si	Mn	P	S	Ni
Wt per cent	0.06	0.17	0.54	0.005	0.006	9.10

Static Yield Stress MPa	Static U. T. S. MPa	Cyclic Yield Stress MPa	Elongation %
698	745	436	37.0

Table 2

Specimen \ Position	B1	B2	S1	W	SL
Type 1	70.6 MPa	68.6 MPa	11.8 MPa	39.2 MPa	58.8 MPa
Type 2	———	———	117.6	58.8	120.6

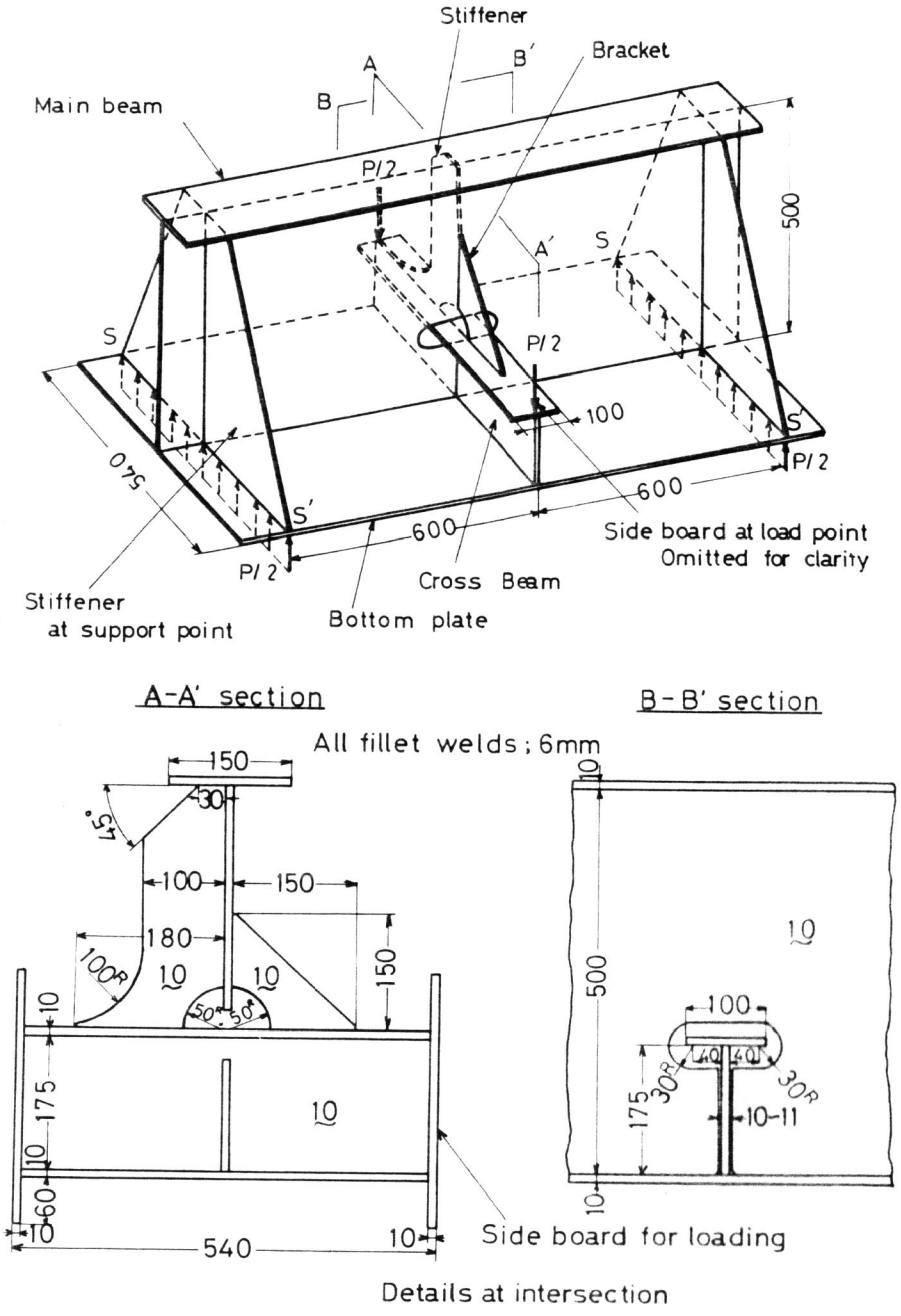

Figure 1 Details of Beam Specimens of Type 1

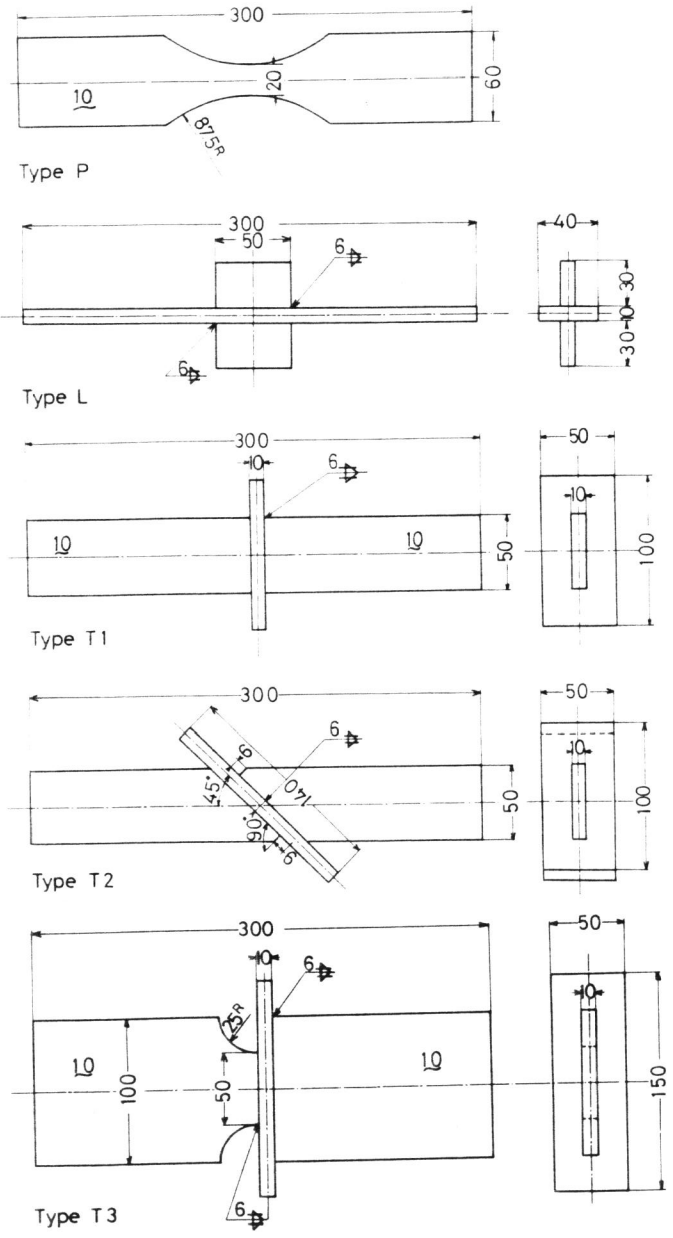

Figure 2 Details of Plate Specimens

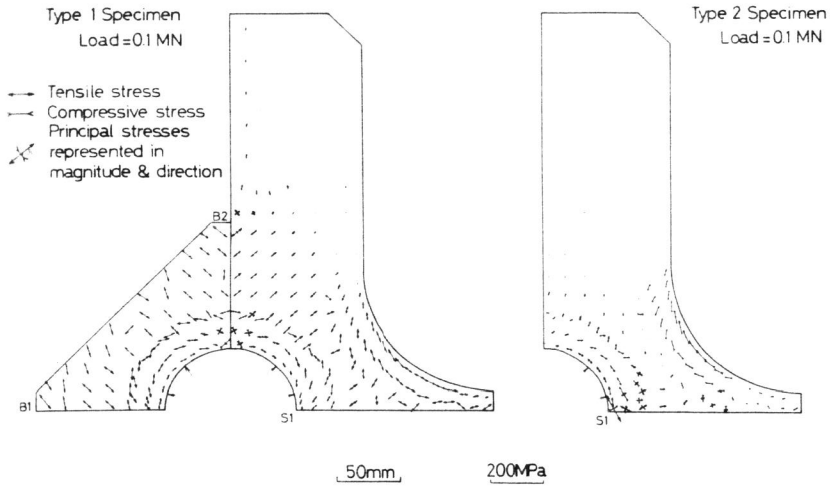

Figure 3 Distribution of Principle Stresses in Stiffener and Bracket for Type 1 Specimen and in Stiffener for Type 2 Specimen (computation by FEM)

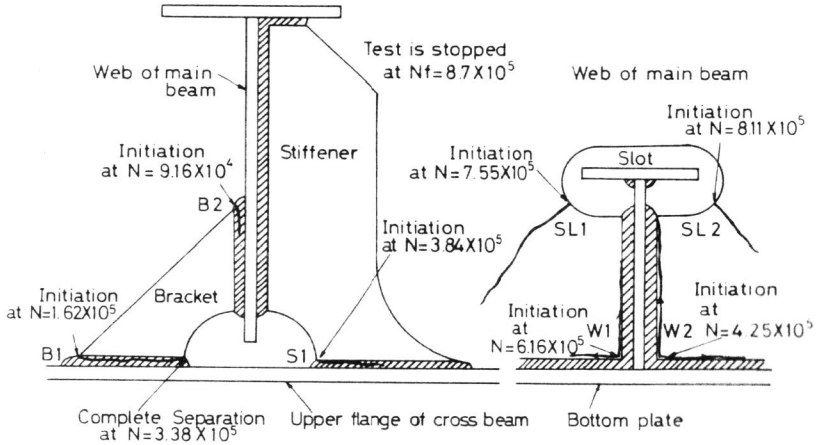

Figure 4 Behaviour of Fatigue Cracks in the Intersecting Part of Main Beam/Cross Beam for Type 1 Beam (Load = 0.37 MN)

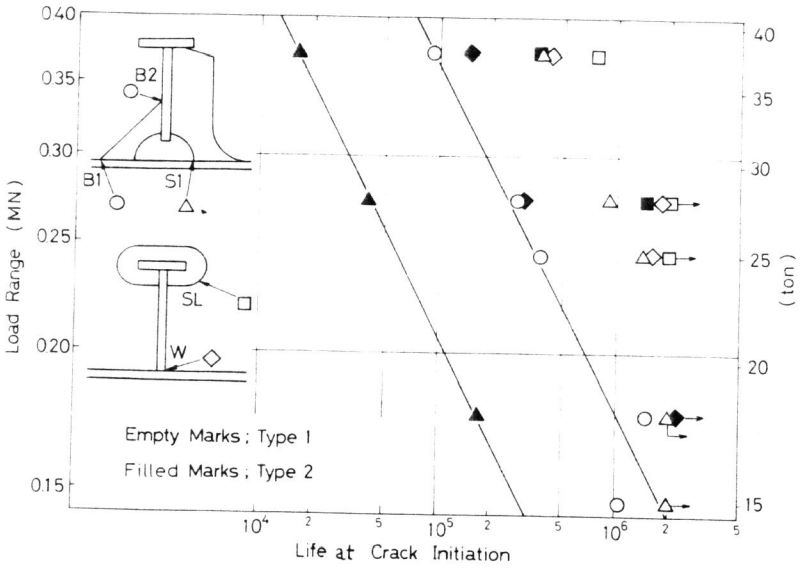

Figure 5 Fatigue Test Results for Beam Specimens

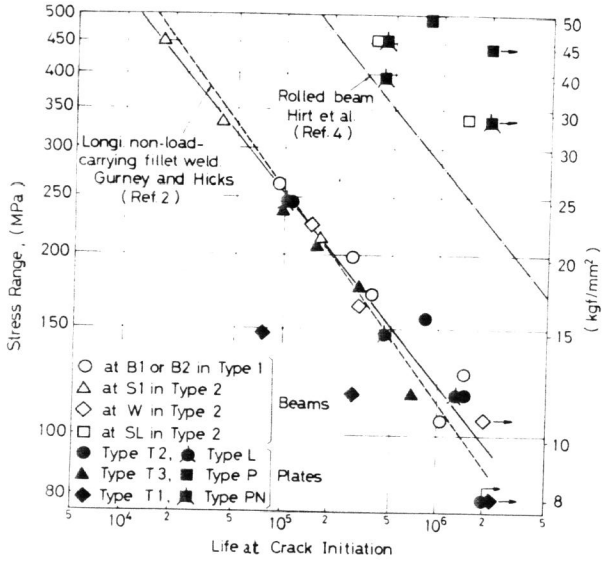

Figure 6 SN Relationships for Beam Specimens and for Plate Specimens